

Joint Institute for Nuclear Research

Bogoliubov Laboratory
50 years

Ed. D. V. Shirkov

Dubna 2006

Towards Searching for a Mixed Phase of Strongly Interacting QCD Matter at the JINR Nuclotron

A. N. Sissakian^a, A. S. Sorin^a, M. K. Suleymanov^b,
V. D. Toneev^a, and G. M. Zinovjev^c

^a*Bogoliubov Laboratory of Theoretical Physics,
Joint Institute for Nuclear Research, Dubna, Russia*

^b*Veksler and Baldin Laboratory of High Energies,
Joint Institute for Nuclear Research, Dubna, Russia*

^c*BITP NAS, Kiev, Ukraine*

Abstract

Available experimental data in respect to a possible formation of a strongly interacting mixed phase are outlined. A physical program is formulated for new facilities being opened in Dubna for acceleration of heavy ions with an energy up to 5 AGeV.

Over the last 25 years a lot of efforts have been made to search for new states of strongly interacting matter under extreme conditions of high temperature and/or baryon density, as predicted by Quantum Chromodynamics (QCD). These states are relevant to understanding the evolution of the early Universe after Big Bang, the formation of neutron stars, and the physics of heavy-ion collisions. The latter is of great importance since it opens a way to reproduce these extreme conditions in the Earth laboratory. This explains a permanent trend of leading world research centers to construct new heavy ion accelerators for even higher colliding energy.

Looking at the list of heavy-ion accelerators one can see that after the first experiments at the Dubna Synchrophasotron, heavy-ion physics successfully developed at Bevalac (Berkeley) with the bombarding energy to $E_{lab} \sim 2$ AGeV, AGS (Brookhaven) $E_{lab} \sim 11$ AGeV, and SPS (CERN) $E_{lab} \sim 160$ AGeV. The first two machines are closed now. The nuclear physical programs at SPS as well as at SIS (GSI, Darmstadt, $E_{lab} \sim 1$ AGeV) are practically completed. The new relativistic heavy-ion collider (RHIC, Brookhaven) is intensively working in the ultrarelativistic energy range $\sqrt{s_{NN}} \sim 200$ GeV to searching for signals of the quark-gluon plasma formation. In this respect, many hopes are related to the Large Hadron Collider (LHC, CERN) which will start to operate in the TeV

region in two-three years. The low-energy scanning program at SPS (NA49 Collaboration) revealed an interesting structure in the energy dependence of some observables at $E_{lab} \sim 20 - 30$ AGeV, which can be associated with the exit of an excited system into a deconfinement state. This fact essentially stimulated a new large project FAIR GSI (Darmstadt) for studying compressed baryonic matter in a large energy range of $E_{lab} = 10 - 30$ AGeV which should come into operation after 2013 year [1]. The general scheme how available accelerators are spread over the world is presented in Fig. 1.

Heavy Ion Accelerators



Fig. 1. The present and future accelerators of relativistic nuclear beams. For each facility the name of the laboratory, the name of the accelerator and the energy range (center-of-mass energy per nucleon-nucleon pair $\sqrt{s_{NN}}$ in GeV) are given [2]

On the other hand, in JINR there is a modern superconducting accelerator, Nuclotron, which has not realized its planned parameters yet. The Veksler and Baldin Laboratory of High Energy has certain experimental facilities and large experience to work with heavy ions. This study may actively be supported by theoretical investigations of the Bogoliubov Laboratory of Theoretical Physics. The paper aims to give an overview of experimental results on manifestation of some peculiarities of strongly interacting QCD matter, observed in relativistic heavy ion collisions, and to present arguments that acceleration of heavy ions like Au at the Nuclotron up to the maximal planned energy $E_{lab} = 5$ AGeV, allows one to study properties of hot and dense QCD matter to be competitive at the world level.

A convenient way to present a variety of possible states of strongly interacting matter is a phase diagram in terms of temperature T and baryon chemical potential μ_B (or baryon density n_B), as shown in Fig. 2. This schematic picture shows in which region of the diagram

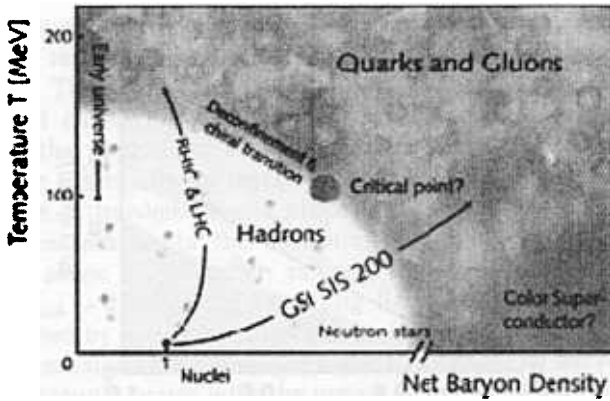


Fig. 2. Artist's view of the phase diagram [1]

the given phase is realized and which colliding energies are needed to populate this region. In particular, the boundary of the deconfinement and/or chiral symmetry restoration transition may be reached even below bombarding energies planned in the FAIR GSI project but the nuclear matter compression should be high enough.

This point is illustrated in more detail in Fig. 3.

As is seen, a system, formed in a high energy collision, is fast heated and compressed and then starts to expand slowly reaching the freeze-out point which defines observable hadron quantities. Indeed, at the maximal achievable Nuclotron energy $E_{lab} = 5$ AGeV the system «looks» into the mixed phase for a short time (the left part of Fig. 3). However, uncertainties of these calculations are still large. If heavy masses for u, d quarks are assumed, the phase boundary is shifted towards higher μ_B (the right part in Fig. 3). On the other hand, these dynamical trajectories were calculated for a pure hadronic gas equation of state, and the presence of a

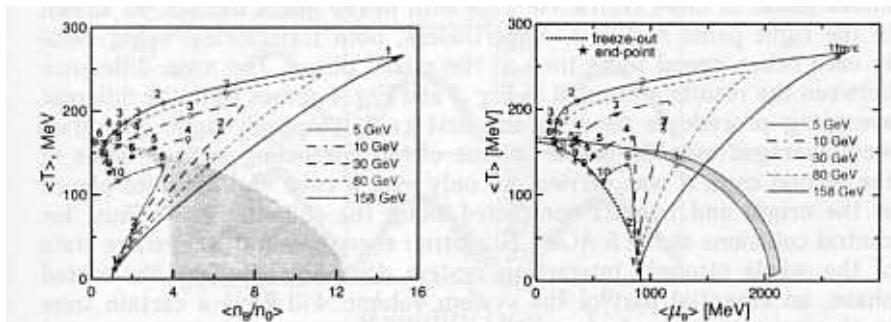


Fig. 3. Dynamical trajectories for central ($b = 2fm$) Au + Au collisions in $T - n_B$ (left panel) and $T - \mu_B$ (right panel) plane for various bombarding energies calculated within the relativistic 3-fluid hydrodynamics [3]. Numbers near the trajectories are the evolution time moment. Phase boundaries are estimated in a two-phase bag model.

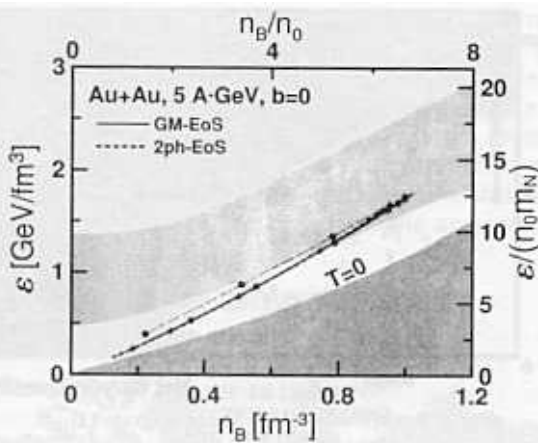


Fig. 4. Dynamical trajectory in the $\varepsilon - n_B$ -plane for central Au+Au collisions calculated with two equations of state: pure hadronic (solid line) and with first order phase transition (dashed). Spatial averaging is done over the cube with the 4 fm sides and Lorentz contracted in the longitudinal direction [6]. The shaded regions correspond to the mixed phase (upper one) and the non-reachable domain with the boundary condition $T = 0$, respectively

phase transition may noticeably change them. In addition, near the phase transition the strongly interacting QCD system behaves like a liquid rather than a gas, as was clarified recently at small μ_B from both quark [4] and hadronic [5] side. As to high μ_B values, it is a completely open question. One should note also that as follows from lattice QCD calculations for $\mu_B \approx 0$ the deconfinement temperature practically coincides with the transition temperature for chiral restoration symmetry while for baryon rich matter it is still an open question.

In Fig. 4, dynamical trajectories in the $\varepsilon - n_B$ plane for the top Nuclotron energy are given for two equations of state, without and with the first order phase transition [3, 6]. The shaded band corresponds to the mixed phase of more restrictive EoS with heavy quark masses, as shown in the right panel of Fig. 3. Nevertheless, both trajectories, being close to each other, spend some time in the mixed phase. The main difference between the results presented in Fig. 3 and Fig. 4 comes from the different averaging procedures used: in the first case, thermodynamic quantities were averaged over the whole volume of the interacting system, while in the second case, it was carried out only over a cube of 4 fm sides placed at the origin and Lorentz contracted along the colliding axis. Thus, for central collisions at the 5 AGeV Nuclotron energy even if an average state of the whole strongly interacting system does not approach the mixed phase, an essential part of the system volume will have a certain time in this mixed phase. An experimental consequence is that an expected observable signal for reaching the mixed phase should be rather weak.

It is hard to believe that some irregular structure like that at $E_{lab} \sim 30$ AGeV [7] can manifest itself at the Nuclotron energy. So the global

observables are expected to be quite smooth with energy. Indeed, as is seen from the results presented in Figs.5 and 6 covering the region of $\sim 2-10$ AGeV. The shape of rapidity spectra for newly produced mesons is bell-like but cannot be described by a single Gaussian due to flow effects. Note that a number of π^+ is not equal to that of π^- though their difference essentially decreases with the bombarding energy. So the isotopic degree of freedom should properly be taken into account under theoretical consideration in the Nuclotron energy range. As to proton spectra, their shape is yet wider, ranging from the target to projectile rapidity. At $E_{lab} \sim 10$ AGeV it is getting flat at the middle rapidity and may be described by a superposition of two Gaussian to SPS energies [3] and of three Gaussian at the RHIC energies. The shape of baryon rapidity distributions strongly varies with the impact parameter (see Fig. 6) taking U-shape for peripheral collisions. The noted trends are continued with increase in energy and governed mainly by the stopping power of colliding matter. To see any effect of phase transformation in a global rapidity distribution, a phase like that should be created in a large volume and should live for a long time. Possibly, it is seen as appearance of the third midrapidity source at the RHIC energies [10].

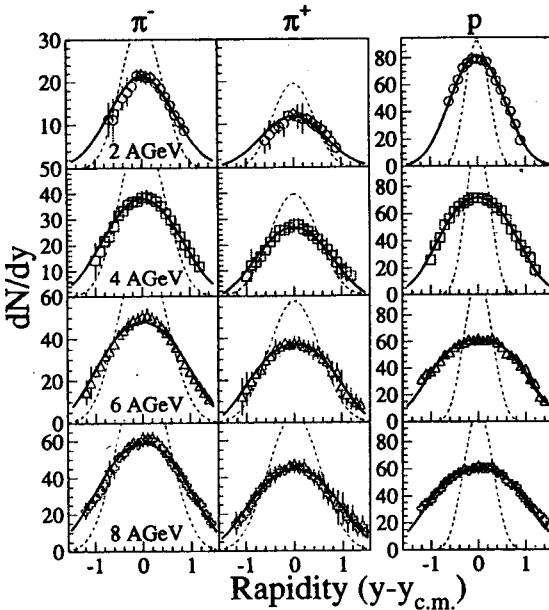


Fig.5. The π^+ , π^- and proton rapidity distributions in central Au+Au collisions at bombarding energies 2, 4, 6, and 8 AGeV [8]. Solid lines are drawn along experimental points. For comparison, Gaussian distributions are given by dashed curves

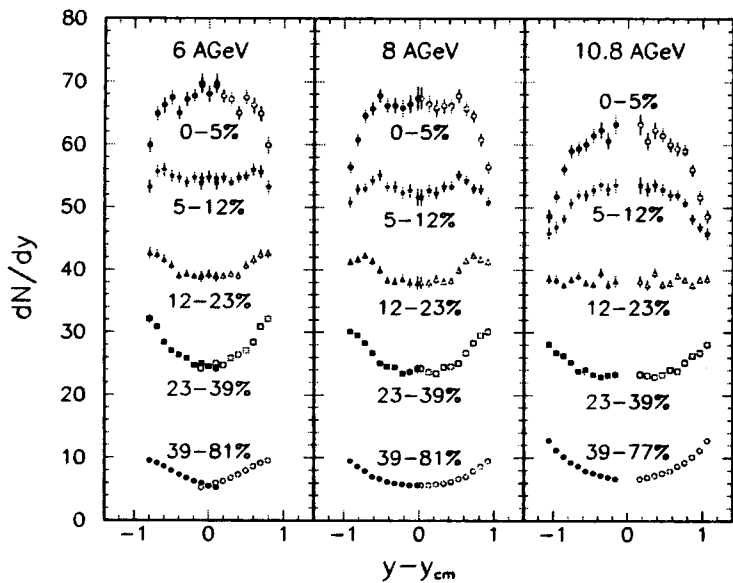


Fig. 6. Proton rapidity distributions for different centrality of Au+Au collisions at 6, 8, and 10.8 AGeV [9]. Filled symbols are measured points, empty ones are their reflection with respect to the $y = y_{cm}$ line. Numbers under distributions give the centrality percentage

Thus, sensitivity of global observables to possible phase transitions is expected to be weak, but it might not be the case for more delicate characteristics. In any case, due to the proximity of the phase diagram region under discussion to the confinement transition and chiral symmetry restoration, some precursory phenomena cannot be excluded at a bombarding energy of about 5 AGeV, which opens a new perspective for physical investigations at the Dubna Nuclotron.

Below some arguments in favor of this statement are given:

- Properties of hadrons are expected to change in hot and/or dense baryon matter [11, 12]. This change concerns hadronic masses and widths, first of all for the σ -meson as the chiral partner of pions which characterizes a degree of chiral symmetry violation and can serve as a «signal» of its restoration as well as the mixed phase formation. Rare decays in matter of vector mesons (particularly ρ and ω) are also very attractive.

The presence of in-medium modification of ρ -mesons has been proved in the CERES experiments, see an example in Fig. 7. The observed essential enhancement of low-mass ($0.2 \lesssim M \lesssim 0.7$) lepton pairs, as compared to free hadron decays, is due to the influence of hot and dense nuclear matter on properties of the ρ -meson spectral function. Both the Brown-Rho scaling hypothesis [12] assuming a dropping ρ mass and a strong broadening, as found in the many-body approach by Rapp and Wambach [14], result in

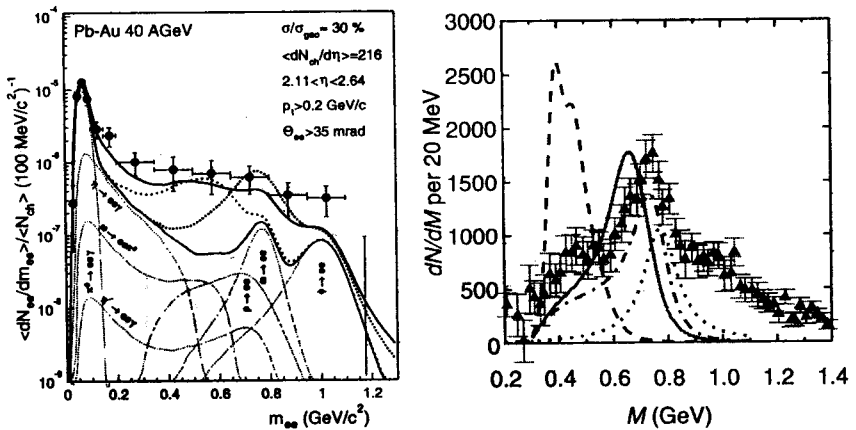


Fig. 7. Left panel: e^+e^- invariant spectra from central $Pb + Au$ (40 GeV) collisions [13]. Thin solid and dotted lines are hadronic cocktail and the calculated results for free ρ mesons, respectively. Appropriate thick solid and dash-dotted lines are calculated in the Rapp-Wambach [14] and Brown-Rho [12] scenarios. Contributions of different channels are shown as well. Right panel: Invariant mass distribution of dimuons from semi-central In+In collisions at the beam energy 158 AGeV. Experimental points are from [15]. Solid and dashed curves are calculated [16] in the dropping mass scenario using the ρ -mass modification factors as density and temperature-density dependent, respectively. Dash-dotted curve neglects any in-medium modification. Dotted line indicates the hydrodynamically calculated ρ -meson decay at the freeze-out

reasonable agreement with experiment. However, a poor resolution in the dielectron mass prevents the discrimination of different physical scenarios of this effect in the CERES experiments. The situation is noticeably better in the recent NA60 experiment with muon pairs [15]. As is seen from the right panel of Fig.7, the quality of dimuon data is much higher allowing a good resolution of the spectral function. The depicted comparison with the dropping mass scenario shows a strong influence of the final result on the hypothesis used for in-medium dependence of the mass modification factor [16]. However, it seems to be impossible to describe simultaneously dielectron and dimuon experimental data within the dropping mass scenario under the same assumptions. Similar data are absent for heavy ions in the Nuclotron energy range.

As to in-medium σ -meson decay, some indications were obtained in reactions induced by pions and photons [17–19]. In Fig. 8, the relative pion pair abundance $C_{\pi\pi}^A$, defined as

$$C_{\pi\pi}^A = \frac{\sigma^A(M_{\pi\pi})}{\sigma_T^A} / \frac{\sigma^N(M_{\pi\pi})}{\sigma_T^N},$$

is presented for different isotopic states of observed pions versus the invariant pion pair mass $M_{\pi\pi}$. A sizable enhancement is observed at

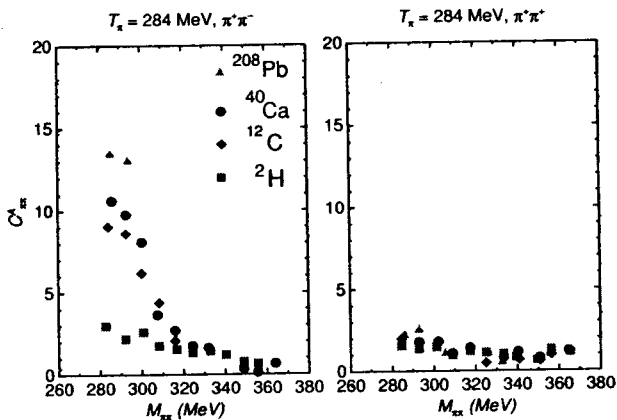


Fig. 8. Invariant mass distribution of pion pairs from π -nucleus interactions [17]

low $M_{\pi\pi}$ in the case of $\pi^+ \rightarrow \pi^-\pi^-$ reaction but not for the $\pi^+ \rightarrow \pi^+\pi^+$ case [17]. This enhancement may be related to a possible $\pi\pi$ scattering in a nucleus via formation of a virtual scalar σ meson which is forbidden for the $\pi^+\pi^+$ state. The effect is getting stronger for heavier nuclei. Recently, using the ELSA tagged facilities in Bonn the in-medium modification of the ω -meson has first been observed in the reaction $\gamma + A \rightarrow \omega + X \rightarrow \pi^0 + \gamma + X$ [19]. A small shift in the ω mass was detected. Note, however, that in π^- - and

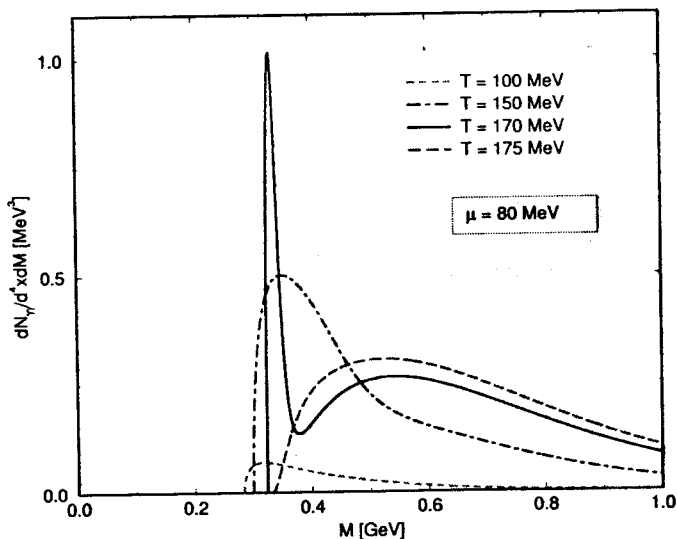


Fig. 9. Invariant mass spectra of 2γ at $\mu_B = 80$ MeV and different temperatures [21].

γ -induced reactions we deal with comparatively low baryon density states, $n_B \sim (1 - 2)n_0$. There are no similar experiments with heavy ions.

Nevertheless, there are theoretical proposals to probe chiral symmetry restoration in the vicinity of the phase transition boundary. In particular, it was shown [20,21] that a two-photon decay of the σ -meson formed as an intermediate state in $\pi\pi$ scattering may be a very attractive signal. As depicted in Fig. 9, at temperature in the vicinity of the phase transition, when $m_\sigma \sim 2m_\pi$, there is an anomalous peak in invariant mass spectra of γ pairs which may serve as a signal of the phase transition and formation of a mixed phase. Certainly, there is a huge combinatorial background due to $\pi^0 \rightarrow \gamma\gamma$ decays, but the Nuclotron energy is expected to have some advantage against higher energy accelerators because the contribution of deconfined quarks-gluons will be negligible.

This effect may be observed in the e^+e^- decay channel as well [22].

- Electromagnetic probes discussed above carry out information concerning the whole evolution of colliding nuclei and states which are realized. The bulk of produced hadrons is related to the freeze-out point where information on the interaction dynamics has essentially been erased. So the expected behavior of global hadronic observables is smooth. However, some peculiarities of delicate hadron characteristics may be found and their hints are available even now.

In Fig. 10, the beam energy dependence of the elliptic flow coefficient v_2 is presented for protons in the midrapidity range from noncentral heavy-ion collisions [23]. The elliptic flow characterizes the angular anisotropy in the transverse momentum plane as

$$dN/d\phi \sim [1 + 2v_1 \cos(\phi) + 2v_2 \cos(2\phi)] ,$$

where the ϕ angle is measured from the reaction plane. As is seen, just near the Nuclotron energy $E_{lab} \sim 5$ AGeV the coefficient v_2 changes its sign and the transverse flow evolves from the out-of-plane towards in-plane emission. This fact may be treated as softening of the equation of state to be a precursor of the phase transition. The elliptic flow shows an essentially linear dependence on the impact parameter with a negative slope at $E_{lab} = 2$ AGeV, with a positive slope at 6 AGeV and with a near zero slope at 4 AGeV [24]. This dependence serves as an important constraint to high-density behavior of nuclear matter for discrimination of various equations of state.

- Strangeness enhancement is an intriguing point of physics of heavy ion collisions, being one of the first proposed signals of quark-gluon plasma formation. An important experimental finding is the observation of some structure («horn») in the energy dependence of reduced strangeness multiplicity at $E_{lab} \sim 30$ AGeV, predicted

Elliptic Flow

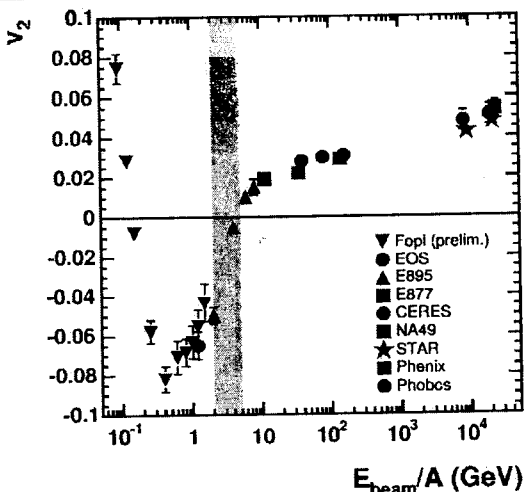


Fig. 10. Excitation function of the proton elliptic flow [23]. The shaded band corresponds to the Nuclotron energy

in [25] as a signal that the formed excited system came into a deconfinement phase. As an example, in Fig. 11 the K^+/π^+ average multiplicity ratio is displayed as a function of the colliding energy.

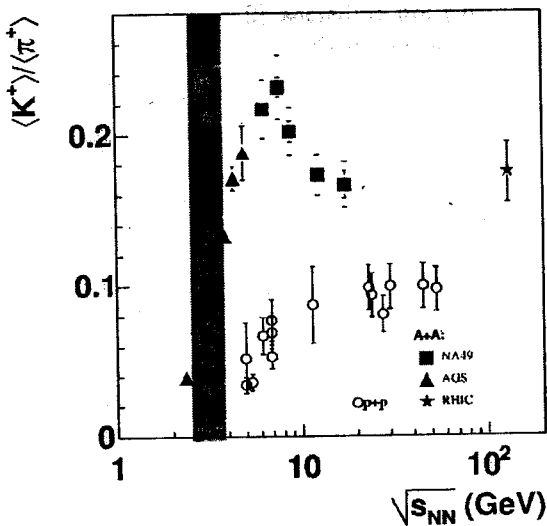


Fig. 11. Colliding energy dependence of the reduced strangeness abundance of K^+ mesons [26]. The shaded band corresponds to the Nuclotron energy range.

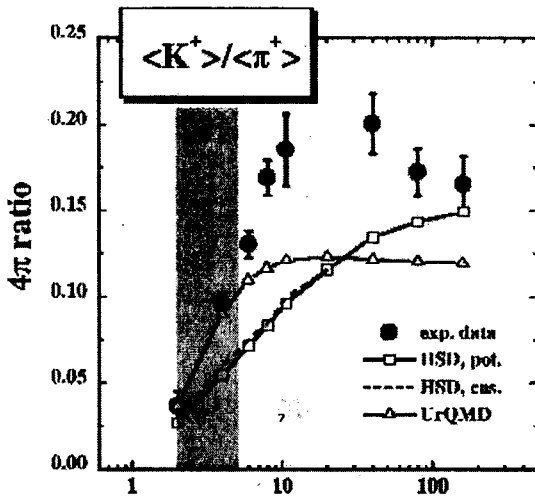


Fig. 12. Beam energy dependence of the K^+/π^+ ratio. Curves are the results of different transport calculations (the figure is taken from [27]). The shaded band corresponds to the Nuclotron energy range

The «horn» structure is well visible. Such a structure is absent in free nucleon-nucleon collisions.

The same experimental data (besides two recent points measured at $E_{lab} = 20$ and 30 AGeV) are plotted in Fig. 12 as a function of the bombarding energy. It is of great interest that these ratios for strange hadrons are not explained by the modern transport theory (UrQMD, HSD models). While the mean pion and kaon multiplicities are well reproduced at the SIS and SPS energies, the

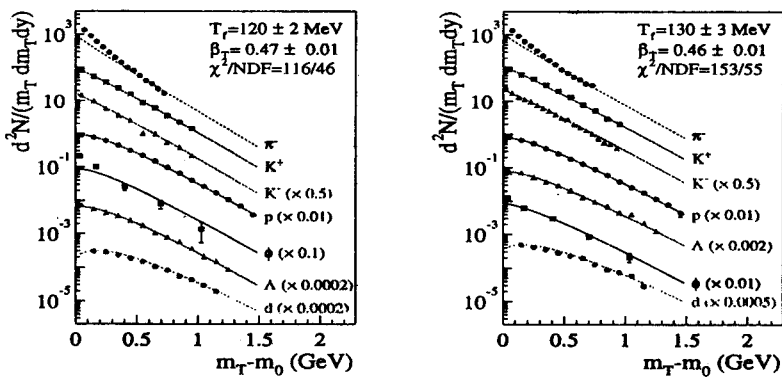


Fig. 13. The transverse mass spectra at midrapidity for different hadrons produced in central Pb+Pb collisions at 20 AGeV and 30 AGeV [26]. Solid lines are results of the blast-wave parameterization[28] with the parameters given in the figure.

above-mentioned models essentially underestimate the K/π ratio in the AGS energy domain. It is remarkable that the divergence between the transport theory and experiment starts just at the Nuclotron energy. This increases interest in future experiments at the Nuclotron.

- A strange particle ratio is not the only attractive observable. Let us look at the Lorentz invariant quantity, the transverse momentum distribution, presented in Fig. 13.

It is a global characteristic and no peculiarities are expected. Indeed, experimental spectra are reasonably well described within a simple blast-wave model [28] where spectra at freeze-out are parameterized as follows:

$$\frac{dN}{dy m_T dm_T} \simeq m_T K_1 \left(\frac{m_T \text{ch } \rho}{T} \right) I_0 \left(\frac{p_T \text{sh } \rho}{T} \right)$$

with the boost angle $\rho = \text{th}^{-1} \beta_T$ and values of the freeze-out temperature T and transverse velocity β_T are given in Fig. 13. However, the behavior of the average transverse mass, $\langle m_T \rangle - m_0$, versus colliding energy \sqrt{s}_{NN} , is not trivial. As follows from Fig. 14, a remarkable change in the energy dependence around a beam energy of ~ 30 AGeV is clearly visible for pions and kaons exhibiting some kind of plateau. While $(\langle m_T \rangle - m_0)$ rises steeply in the AGS energy range, this rise is much weaker from low SPS energies until RHIC energies where it starts again to rise. To a lesser extent this change is also seen for protons. One should emphasize that the beginning of the plateau is well correlated with the «horn» position. Measurements at the Nuclotron may specify a pre-plateau behavior, in particular, for kaons and protons. Among many signals of the formation of Quark Gluon Plasma (QGP), one of the earliest is based on the relation of the

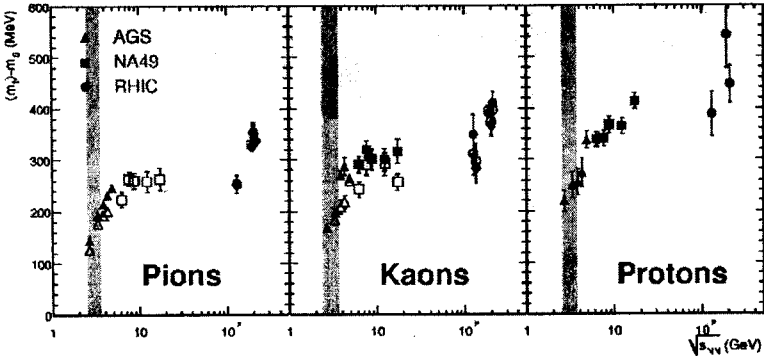


Fig. 14. The energy dependence of $\langle m_T \rangle - m_0$ for pions, kaons, and protons at midrapidity for the most central Pb+Pb/Au+Au collisions [7]. Shaded bands correspond to the Nuclotron energy.

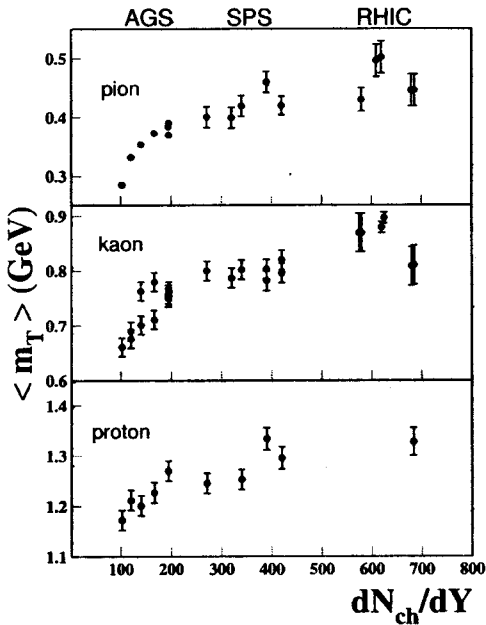


Fig. 15. Variation of $\langle m_T \rangle$ with produced charged particles per unit rapidity at midrapidity for central collisions corresponding to the energy range from AGS to RHIC [30]. The error bars reflect both the systematic and statistical errors in obtaining T_{eff}

thermodynamical variables, temperature, and entropy to the average transverse momentum and multiplicity, respectively, as was originally proposed by Van Hove [29]. It was argued that a plateau in the transverse momentum beyond a certain value of multiplicity would indicate the onset of the formation of a mixed phase of QGP and hadrons, similar to the plateau observed in the variation of temperature with entropy in a first order phase transition scenario. In Fig. 15, the variation of $\langle m_T \rangle$ with charged multiplicity produced per unit rapidity dN/dy around the midrapidity [30] is depicted for pions, kaons, and protons at AGS, SPS and RHIC energies spanning the range from 2 AGeV to 200 AGeV. In this analysis the experimental data on transverse mass spectra were parameterized as

$$\frac{dN}{m_T dm_T} \simeq C \exp(-m_T/T_{eff}) \quad (1)$$

with the inverse slope parameter treated as an effective temperature T_{eff} . The average transverse mass of hadrons is related with T_{eff} :

$$\langle m_T \rangle = T_{eff} + m + \frac{(T_{eff})^2}{m + T_{eff}}$$

From the results shown in Fig. 15 one observes an increase in $\langle m_T \rangle$ with a particle density dN_{ch}/dy for AGS energies followed by a plateau for charge multiplicities corresponding to SPS energies for all the particle types considered: pions, kaons and protons. This may hint at the mixed phase, possible co-existence of the quark and hadron phases. For charge multiplicities corresponding to higher RHIC energies, the $\langle m_T \rangle$ shows an increasing trend indicating the possibility of a pure QGP formation.

Using eq.(1), one may directly analyze data in terms of effective temperature. As is shown in Fig. 16, the inverse slope parameter of kaons increases in the AGS and RHIC energy domains but it stays constant at SPS energies in natural agreement with the particle ratio results presented above. This feature, which is not observed in $p + p$ interactions, might be attributed to the latent heat of a phase transition [31] and it is in fact consistent with hydrodynamic model calculations assuming a first order phase transition [32].

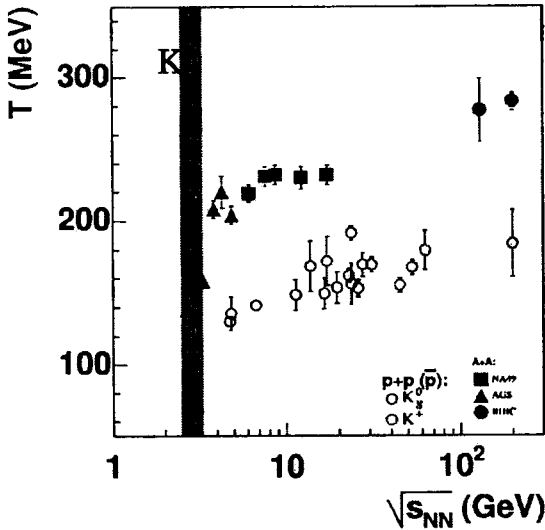


Fig. 16. The energy dependence of the inverse slope parameter of kaons [7]. The shaded band corresponds to the Nuclotron energy

- As mentioned above, global multiplicities are expected to be quite smooth over a large range of energy. Fig. 17 shows the mean multiplicities of hadrons emitted in central Pb+Pb/Au+Au collisions as a function of energy. The results are well described within the statistical hadron gas model [33]. Note that a number of charged pions ($n_{\pi^+} + n_{\pi^-}$) ~ 150 and kaons $K^+ \sim 7$ per central event at the top Nuclotron energy.

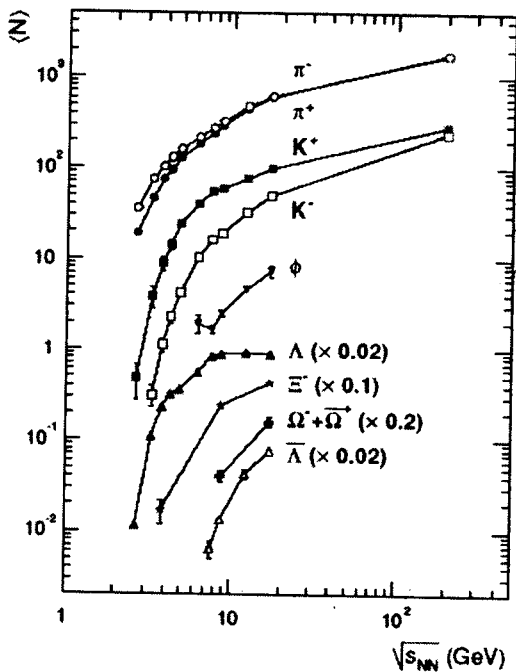


Fig. 17. The colliding energy dependence of the mean multiplicities of various hadrons emitted in central Pb+Pb/Au+Au collisions [33].

However one should add that peculiarities at the «horn» energy in strange particle ratios and the effective temperature dependence are also observed in average pion number per nucleon-nucleon interaction [7]. Such an example is given in Fig. 18:

The reduced pion multiplicity $\langle n_\pi \rangle / A_{part}$ for nucleus-nucleus collisions is below that for elementary NN interactions at moderate energies and exceeds appropriate NN values in a relativistic domain. According to [7,25], the equality of the nuclear and elementary $\langle n_\pi \rangle / A_{part}$ ratios at the «horn» energy is treated as an argument in favor of the onset of deconfinement. However, this proximity of nuclear and elementary reduced pion multiplicities starts at the Dubna Nuclotron energy and could naturally be explained by the role of the Δ isobar in the pion absorption. To clarify this or alternative interaction mechanisms, new experimental data for heavy ion collisions with scanning over the Nuclotron energy range are needed.

- Existing experimental data indicate a large degree of equilibration of nuclear matter from high-energy heavy-ion collisions at freeze-out (see review-article [35]). The results presented in Fig.19 demonstrate a high quality description of relative hadron yields

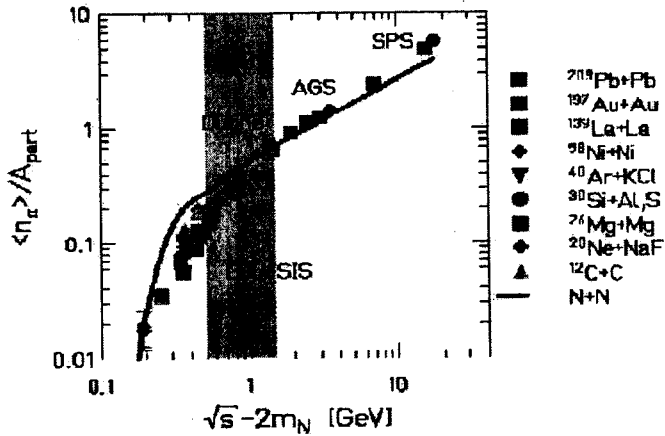


Fig. 18. Pion multiplicity per participating nucleon for nucleus-nucleus (symbol) and nucleon-nucleon collisions (solid line) as a function of available energy in nucleon-nucleon collisions [34] The shaded band corresponds to the Nuclotron energy

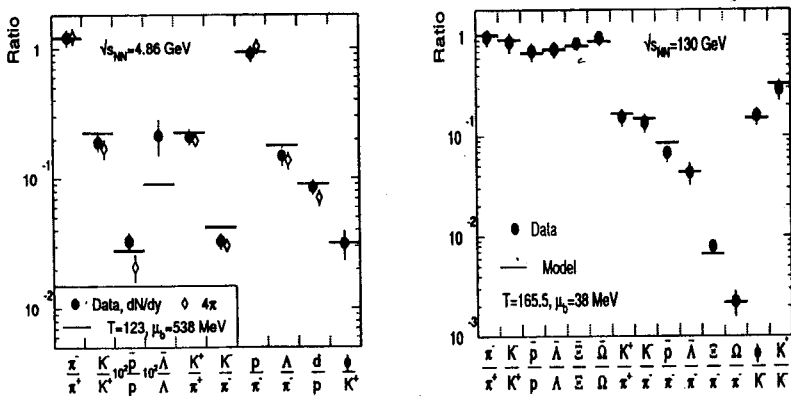


Fig. 19. Yield ratios with the best fit at midrapidity for the top AGS beam energy 10.7 AGeV (left panel) and for the RHIC colliding energy $\sqrt{s_{NN}} = 130$ GeV (right panel) [36]. The diamonds represent ratios of yields integrated over 4π . Note the scaling factor 100 for the ratios \bar{p}/p and $\bar{\Lambda}/\Lambda$ in the left figure. The extracted freeze-out temperature and baryon chemical potential are displayed in the figures

within the equilibrium statistical model obtained by means of fitting the temperature and baryon chemical potential.

The mechanisms of equilibration are still unclear. In particular, a large difference between dynamical and statistical models is observed for heavy baryons (e.g. for $\bar{\Lambda}$, multi-strange hyperons, Ξ and Ω^- and resonances) measured at high energies. The role of multiparticle interactions is also obscure. The corresponding data

for the Nuclotron energies are extremely poor. Future Nuclotron measurements could give a strong input for a further development of dynamical and statistical approaches and allow one to disentangle these two types of models.

- To a certain extent, the study of fluctuations in relativistic strongly interacting matter may help with solving the equilibration problem mentioned above. Experimental data on event-by-event fluctuations (e.g., fluctuations of particle multiplicity, electric, baryon and strangeness charges) in nuclear collisions give a unique possibility to test recent ideas on the origin of fluctuations in relativistic interacting systems [37, 38]. Among them suppression of event-by-event fluctuations of electric charge was predicted [37] as a consequence of deconfinement. Estimates of the magnitude of the charge fluctuations indicate that they are much smaller in a quark-gluon plasma than in a hadron gas. Thus, naively, a decrease of the fluctuations is expected when the collision energy crosses the threshold for the deconfinement phase transition. However, this prediction is derived under assumptions that initial fluctuations survive through hadronization and that their relaxation times in hadronic matter are significantly longer than in the hadronic stage of the collision [37, 39]. The magnitude of the measured charge fluctuations depends not only on the unit of electric charge q carried by degrees of freedom of the system (integer charge of hadrons or fractional one of quarks), but also on trivial effects, which may obscure the physics of interest (the fluctuations in the event multiplicity, caused by the variation of the impact parameter, and changes in the mean multiplicity due to changes of the acceptance). In our example, $\Delta\Phi_q$ is used as a measure of charge fluctuation which is constructed from the well established measure Φ_q of event-by-event fluctuations, defined as:

$$\Phi_q = \sqrt{\langle Z^2 \rangle / \langle N \rangle} - \sqrt{z^2}$$

where: $z = q - \bar{q}$, $Z = \sum_{i=1}^N (q_i - \bar{q})$. In these equations N is the number of particles of the given event within the acceptance, and over-line and $\langle \dots \rangle$ denote averaging over a single particle inclusive distribution and over all events, respectively.

For a scenario, in which particles are correlated only by global charge conservation (GCC), the value of Φ_q is given by $\Phi_{q,GCC} = \sqrt{1 - P} - 1$ where $P = \langle N_{ch} \rangle / \langle N_{ch} \rangle_{tot}$ with $\langle N_{ch} \rangle$ and $\langle N_{ch} \rangle_{tot}$ being the mean charged multiplicity in the detector acceptance and in full phase space (excluding spectator nucleons), respectively. In order to remove the sensitivity to GCC, the measure $\Delta\Phi_q$ is defined as the difference

$$\Delta\Phi_q = \Phi_q - \Phi_{q,GCC} .$$

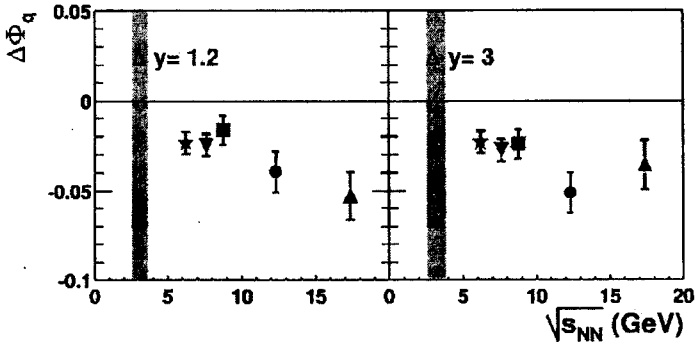


Fig. 20. The colliding energy dependence of $\Delta\Phi_q$ for a small $\delta y = 1.2$ and large $\delta y = 3$ rapidity interval for central $Pb + Pb$ collisions [40]. Shaded bands correspond to the Nuclotron energies

By construction, the value of $\Delta\Phi_q$ is zero if the particles are correlated by global charge conservation only. It is negative in the case of an additional correlation between positively and negatively charged particles, and it is positive if the positive and negative particles are anticorrelated [39].

As is seen from the results presented in Fig. 20, the measured values of $\Delta\Phi_q$ vary between 0 and -0.05. They are significantly larger than those expected for QGP fluctuations $-0.5 < \Delta\Phi_q < -0.15$. A weak decrease of $\Delta\Phi_q$ with increasing energy is suggested by the presented data.

Measurements require tracking detectors of large acceptance and precise control of collision centrality on event-by-event basis. Up to now only results on very limited acceptance at high energies are available, thus new measurements at the Nuclotron energy are of particular importance.

From the experimental point of view the Nuclotron energy range seems to be ideal for these measurements. This is because moderate particle multiplicity and their relatively broad angular distribution simplify an efficient detection of all produced charged particles.

- An investigation of the narrow Hanbury-Brown-Twiss correlations [41] joins this problem. Momentum correlations between mesons have been widely used to study the space-time extent of the emitting source in nucleus-nucleus collisions. For identical bosons the symmetry requirement of the Bose-Einstein statistics results in an enhanced production of bosons with a small momentum difference. Kopylov and Podgoretsky [42] first noticed the deep analogy of this effect with Hanbury-Brown and Twiss space-time correlations of the classical electromagnetic fields used in astronomy for interferometric measurement of star angular radii and developed the basic methods of momentum interferometry in particle and nuclear collisions. This technique represents an

important tool for investigating the underlying reaction mechanism as far as it influences the decoupling configuration, including an unusually long decoupling time suggested as one of the signatures of quark-gluon plasma formation [43].

The correlation function $C_2(p_1, p_2)$ is defined as the ratio of the probability of observing particles with four-momenta p_1 and p_2 simultaneously in one event divided by the probability for pairs of independent particles with the same single particle phase space distribution. In Gaussian approximation with the Bertsch-Pratt parameterization [43] the correlation function may be reduced to

$$C_2(q_{out}, q_{side}, q_{long}) = 1 + \lambda \exp[-q_{out}^2 R_{out}^2 - q_{side}^2 R_{side}^2 - q_{long}^2 R_{long}^2],$$

where q_{long} is the longitudinal momentum component, and (q_{out}, q_{side}) are the components of the transverse 3-momentum difference in an outward direction and perpendicular to it. The parameter λ characterizes the degree of incoherence.

The parameters of the HBT analysis are presented in Fig. 21 as a function of the colliding energy. Although there is some disagreement among experiments, the data do not appear to exhibit any sharp discontinuities but rather smoothly vary as a function of the collision energy. The detailed predictions of Gyulassy and Rischke [45] about a slowly burning quark-gluon plasma have obtained a lot of experimental attention. Namely, it was expected that the HBT radius in the out direction will exceed the HBT radius in the side direction, predicting $R_{out}/R_{side} > 1$ values reaching up to 4 or even 20 in case of an ideal first order phase transition[45]. In contrast, as is seen from Fig. 21, $R_{out} \approx R_{side} \approx R_{long}$ in the RHIC energy region.

The correlation function parameters may be related to physical ones characterizing the system size, lifetime, freeze-out duration, and expansion time. In particular, based on a hydrodynamic expansion model it was shown that $R_{long} = \tau_f \sqrt{\frac{T}{m_T}}$ [46], where τ_f and T are the freeze-out time and temperature of the particles, respectively. One should emphasize that all these investigations suppose that centrality of heavy-ion collisions is under control and centrality scanning of the characteristics under discussion is an indispensable condition.

Measurements of these quantities at the Nuclotron energies should be considered as a necessary continuation of global efforts to establish the energy dependence of properties of hadron production and search for signals of a phase change in nuclear collisions.

In this connection the following theoretical and experimental studies at JINR are considered as perspective [47]:

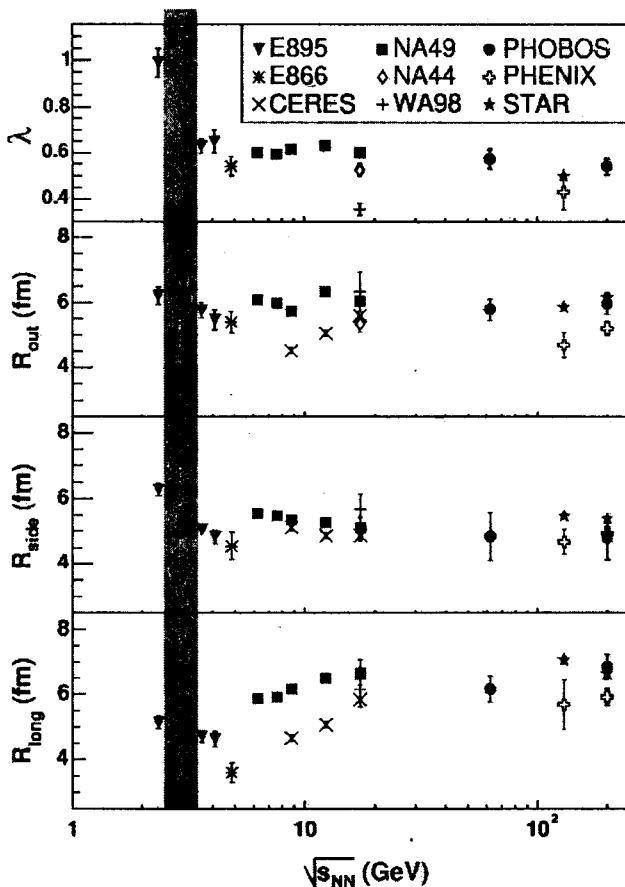


Fig. 21. Bertsch-Pratt parameters as a function of colliding energy for $\pi^-\pi^-$ pairs from central Pb+Pb/Au+Au collisions [44]. The presented data are near midrapidity and for comparable transverse momentum bins from nine different experiments. Systematic errors are not shown.

- 1) research into the hadron properties in hot and/or dense baryonic matter. A spectral function change is expected, first of all for the σ -meson as a chiral partner of pions, which characterizes a degree of chiral symmetry violation. The rare specific channels of ρ -meson decays are also quite attractive.

Solving these issues assumes a proper understanding of reaction mechanisms of high-energy colliding ions, knowledge of properties of strongly interacting QCD matter and its equation of state. In this respect, more general researches are in order:

- 2) analyzing multiparticle hadron interactions, targeted to the development of a new statistical treatment as well as codes for

space-time evolution of heavy nuclei collisions at high energies. Particular attention should be paid to signals of a new phase formation during this evolution;

- 3) studying the system size, lifetime, freeze-out duration, expansion time in the HBT analysis, scanning in atomic number and energy;
- 4) analyzing the energy and centrality dependencies of the pion, hadron resonance and strange particle multiplicities, and the ratio of their yields, together with the transverse momentum, including K^- , K^+ and ϕ -meson spectra as well as manifestation of baryon repulsion effects on hadron abundances;
- 5) studying dileptons (electron and muon pairs) production to see in-medium modification of hadron properties at high baryon densities;
- 6) studying angular correlations in the transverse plane as well as radial, directed and elliptic flows;
- 7) analyzing fluctuations of multiplicities, electric charge, and transverse momenta for secondary particles (their energy dependencies could give information on the phase transition range);
- 8) analyzing nuclear fragments characteristics versus centrality, universality of nuclear fragmentation;
- 9) energy and atomic number scanning for all characteristics of central heavy nuclei collisions (this might allow one to obtain information on the equation of state of strongly interacting QCD matter in the transition region), difference between central collisions of light nuclei and peripheral heavy ion collisions.

The JINR Nuclotron has a possibility to accelerate heavy ions (up to $A > 200$) to the maximal energy of 5 AGeV in about a year. Quite recently it appeared that the projected energy of the nuclotron accelerator complex can be radically increased up to 25 GeV/nucleon. Technical realization of this possibility will be an important task for the next 5-6 years. This gives a chance to address experimentally many recent problems before the FAIR GSI accelerator comes into operation. The proposed research program at the Nuclotron may be considered as a pilot study preparing for subsequent detailed investigations at SIS-100/300 [1] and as an integral part of the world scientific cooperation to study the energy dependence of hadron production properties in nuclear collisions.

Acknowledgements We greatly appreciate many useful and valuable discussions with M. Gazdzicki, M. Gorenstein, H. Gutbrod T. Hatsuda, T. Kunihiro, H. Satz, and H. Ströbele. We are thankful to V.V. Skokov for help in preparing the manuscript. This work was supported in part by RFBR Grant N 05-02-17695 and by the special program of the Ministry of Education and Science of the Russian Federation (grant RNP.2.1.1.5409).

References

1. Proposal for an International Accelerator Facility for Research with Heavy Ions and Antiprotons, <http://www.gsi.de/documents/DOC-2004-Mar-196-2.pdf>.
2. M. Gazdzicki, arXiv:nucl-ex/0512034.
3. Y.B. Ivanov, V.N. Russkikh and V.D. Toneev, Phys. Rev. C **73**, (2006) 044904 [arXiv:nucl-th/0503088].
4. E.V. Shuryak and I. Zahed, hep-ph/0307267.
5. D.N. Voskresensky, Nucl. Phys. A **744** (2004) 378 [arXiv:hep-ph/0402020]; G.E. Brown, Ch.-H. Lee, and M. Rho, A new state of matter at high temperature as "sticky molasses", arXiv:hep-ph/0402207.
6. Yu. Ivanov, Multi-fluid hydrodynamics, Talk at the CBM Collaboration Meeting "FAIR, The physics of compressed baryonic matter", December 15-16, 2005, GSI, Darmstadt, <http://www.gsi.de/documents/DOC-2005-Dec-112-1.pdf>; V.N. Russkikh, private communication.
7. M. Gazdzicki, arXiv:nucl-ex/0507017; C. Blume (NA49 Collaboration), [arXiv:hep-ph/0505137].
8. J.L. Klay et al. Phys. Rev. C **68**, 054905 (2003) [arXiv:nucl-ex/0306033].
9. B. Holzman et al. Nucl. Phys. A **698** 643 (2002) [arXiv:nucl-ex/0103015].
10. G. Wolschin, arXiv:hep-ph/0509108.
11. T. Hatsuda and T. Kunihiro, Phys. Rep. **247** (1994) 221.
12. G.E. Brown and M. Rho, Phys. Rep. **269**, (1996) 333.
13. D. Adamova et al., CERES/NA45 Collaboration, arXiv:nucl-ex/0209024.
14. R. Rapp and J. Wambach, Adv. Nucl. Phys. **25**, (2000) 1.
15. S. Scomparin et al., QM 2005 Proceedings (2005); S. Damjanovic et al., QM 2005 Proceedings (2005) [arXiv:nucl-ex/0510044].
16. V.V. Skokov and V.D. Toneev, Phys. Rev. C **73**, (2006) 021902 [arXiv:nucl-th/0509085].
17. F. Bonutti *et al.*, (CHAOS Collaboration), Phys. Rev. Lett. **77**, (1996) 603; Nucl. Phys. A **677** (2000) 213.
18. A. Starostin *et al.*, Crystal Ball Collaboration, Phys. Rev. Lett. **85** (2000) 5539.
19. CBELSA/TAPS Collaboration, nucl-ex/0504010.
20. S. Chiku and T. Hatsuda, Phys. Rev. D **58**, 076001 (1998) [hep-ph/9809215]; T. Hatsuda, T. Kunihiro and H. Shimizu, Phys. Rev. Lett. **82**, (1999) 2840.
21. M.K. Volkov, E.A. Kuraev, D. Blaschke, G. Röpke and S.M. Schmidt, Phys. Lett. B **424**, (1998) 235 [hep-ph/9706350].
22. H.A. Weldon, Phys. Lett. B **274** (1992) 133.
23. R. Stock, arXiv:nucl-ex/0405007.
24. P. Chung et al., arXiv:nucl-ex/0112002.
25. M. Gazdzicki and M. I. Gorenstein, Acta Phys. Polon. B **30**, (1999) 2705 [arXiv:hep-ph/9803462].
26. M. Gazdzicki (for the NA49 collaboration), J. Phys. G **30** (2004), S701.
27. H. Weber, E.L. Bratkovskaya, W. Cassing, and H. Stoecker, nucl-th/0209079.
28. E. Schnedermann and U.W. Heinz, Phys. Rev. C **50**, 1675 (1994) [arXiv:nucl-th/9402018]; E. Schnedermann, J. Sollfrank, U.W. Heinz, Phys. Rev. C **48**, 2462 (1993) [arXiv:nucl-th/9307020].

29. L. Van Hove, Phys. Lett. **B 118**, 138 (1982).
30. B. Mohanty, Jan-e Alam, S. Sarkar, T.K. Nayak, B.K Nandi, Phys. Rev. C **68**, 021901 (2003) [arXiv:nucl-th/0304023].
31. M.I. Gorenstein, M. Gazdzicki, K.A. Bugaev, Phys. Lett. **B567**, (2003) 175 [arXiv:hep-ph/0303041].
32. M. Gazdzicki, et al., Braz. J. Phys. **34**, 322 (2004) [arXiv:hep-ph/0309192].
33. C. Blume. J. Phys. G: Nucl. Part. Phys. **31**, S57 (2005).
34. P. Senger and H. Ströbele, J. Phys. G: Nucl. Part. Phys. **25** (1999) R59.
35. P. Braun-Munzinger, K. Redlich and J. Stachel, in *Quark Gluon Plasma 3* eds. R.C. Hwa and X.N. Wang, World Scientific, Singapore, p.491 [nucl-th/0304013].
36. A. Andronic, P. Braun-Munzinger, J. Stachel, nucl-th/0511071.
37. S. Jeon and V. Koch, Phys. Rev. Lett. **85**, 2076 (2000) [arXiv:hep-ph/0003168].
M. Asakawa, U.W. Heinz and B. Muller, Phys. Rev. Lett. **85**, 2072 (2000) [arXiv:hep-ph/0003169]. E.V. Shuryak and M.A. Stephanov, Phys. Rev. C **63**, 064903 (2001) [arXiv:hep-ph/0010100].
38. V.V. Begun, M.I. Gorenstein, A.P. Kostyk and O.S. Zozulya, Phys. Rev. C **71**, 054904 (2005); A. Keranen, F. Becattini V.V. Begun, M.I. Gorenstein and O.S. Zozulya, J. Phys. G **31**, S1095 (2005); V.V. Begun, M. Gazdzicki, M.I. Gorenstein and O.S. Zozulya, Phys. Rev. C **71**, (2005) 054904.
39. J. Zaranek, Phys. Rev. C **66**, 024905 (2002) [arXiv:hep-ph/0111228].
40. C. Alt et al., Phys. Rev. C **70**, 064903 (2004) [arXiv:nucl-ex/0406013].
41. U.A. Wiedemann and U. Heinz, Phys. Rept. **319**, 145 (1999); T. Csorgo, Heavy Ion Phys. **15**, 1 (2002); R. Lednicky, Phys. At. Nucl. **67**, 72 (2004).
42. G.I. Kopylov and M.I. Podgoretsky, Sov. J. Nucl. Phys. **15** (1972) 219 ; ibid. **18** (1973) 336; Sov. Phys. JEPT **42** (1975); G.I. Kopylov, Phys. Lett. **50** (1974) 472; M.I. Podgoretsky, Sov. J. Part. Nucl. **20** (1989) 266.
43. S. Pratt, Phys. Rev. **D33**, 1314 (1986); G. Bertsch et al., Phys. Rev. **D37**, 1202 (1988).
44. B.B. Back, et al., PHOBOS Collaboration, arXiv:nucl-ex/0409001.
45. D. H. Rischke and M. Gyulassy, Nucl. Phys. **A 597**, 701 (1996) [arXiv:nucl-th/9509040]; ibid. **A 608**, 479 (1996) [arXiv:nucl-th/9606039].
46. A. N. Makhlin and Y. M. Sinyukov, Z. Phys. **C39** 69 (1988).
47. A.N. Sissakian, A.S. Sorin, M.K. Suleymanov, V.D. Toneev, and G.M. Zinovjev, arXiv:nucl-ex/0511018.